Neurocomputing 103 (2013) 50–62

Contents lists available at SciVerse ScienceDirect

Neurocomputing

journal homepage: www.elsevier.com/locate/neucom

Postsynaptic organisations of directional selective visual neural networks for collision detection

Shigang Yue [a,*], F. Claire Rind [b]

[a] School of Computer Science, University of Lincoln, Brayford Pool, Lincoln LN6 7TS, United Kingdom
[b] Institute of Neuroscience, Newcastle University, Newcastle Upon Tyne, NE1 7RU, United Kingdom

ARTICLE INFO

Article history:
Received 17 December 2011
Received in revised form
21 June 2012
Accepted 4 August 2012
Communicated by Dr. A. Belatreche
Available online 22 October 2012

Keywords:
Visual motion
Directional selective neuron
Vision
Postsynaptic
Properties
Collision

ABSTRACT

In this paper, we studied the postsynaptic organisations of directional selective visual neurons for collision detection. Directional selective neurons can extract different directional visual motion cues fast and reliably by allowing inhibition spreads to further layers in specific directions with one or several time steps delay. Whether these directional selective neurons can be easily organised for other specific visual tasks is not known. Taking collision detection as the primary visual task, we investigated the postsynaptic organisations of these directional selective neurons through evolutionary processes. The evolved postsynaptic organisations demonstrated robust properties in detecting imminent collisions in complex visual environments with many of which achieved 94% success rate after evolution suggesting active roles in collision detection directional selective neurons and its postsynaptic organisations can play.

1. Introduction

Road traffic accident fatalities worldwide has reached near 1.3 million in 2011 according to the World Health Organisation (WHO). The number of serious injuries caused by road traffic accidents can be ten time of that number. In theory, all accidents can be avoided. Study showed that more than 90% road accidents are caused by or related to human error. Methods to reliably recognise imminent collisions and deploy measures to mitigate possible damage are the key for saving life and avoiding injuries.

Currently, collision avoidance systems based on radar, (for example, [29,25,1], reviewed by [46]), are offered as pricey options on luxury cars. However, the performance of these systems is not always reliable enough, especially for short ranging and smaller objects (for example, objects are less than 50 m away in distance, size of a 6-year-old child), and their cost is too high for wide use. Vision, which is capable of providing and processing plentiful information, should play a significant role in road collision detection. Unfortunately, conventional computer vision techniques have not been able to recognise collisions from dynamic scenes cheaply and efficiently due to visual complexity of such scenes [22,10,46,26].

On autonomous vehicles, new methods that combine several sensors and information processing techniques have demonstrated their ability of driving autonomously in normal or restricted driving scenarios, for example, Google driverless cars [14]. However, neither of these autonomous cars has been properly challenged with complex collision scenes. New robust and efficient image processing solutions are eagerly needed either as standalone collision detection solutions or as complements to other collision detection techniques.

For many animal species, vision plays a vital role for their survival. The visual systems in insects in particular, with their rapid reactions to dynamic scenes using only a small amount of neurons, are becoming very attractive as sources of inspiration (for example, [20,15,5,6,21,48,11,28,43,49,50,9,31,55,56]).

Recently, several specialized neurons found in animals have been modelled and used for collision detection. For example, an identified neuron in locust, the lobula giant movement detector (LGMD) [30,42,35,37] has been used as the basis for an artificial visual system for collision avoidance in robots [36,6,38,39,41,49,50,54] and more recently in cars [51,43,4].

Directional selective neurons are another type of specialized visual neurons with preference to certain directional motion cues. They have also been found in animals for decades (for example, in insects [16,33,34,7]; in vertebrates [2,3,44,47,12,32,24]), and have been thought to be involved in signalling looming as well [19]. Recent research showed that whole field directional selective

* Corresponding author. Tel.: +44 152 283 7397; fax: +44 152 288 6974.
E-mail addresses: syue@lincoln.ac.uk, shigang.yue@ieee.org, yue.lincoln@gmail.com (S. Yue), claire.rind@newcastle.ac.uk (F.C. Rind).

0925-2312/$ - see front matter © 2012 Elsevier B.V. All rights reserved.
http://dx.doi.org/10.1016/j.neucom.2012.08.027

neurons can be organised for extracting translating visual cues [52], and can be organised with a special structure for collision detection [53]. However, it is not clear whether these directional selective neurons can only be integrated with that special structure for collision detection.

If these direction selective neurons can be organised differently for collision detection, what are the properties of these postsynaptic organisations (i.e., neural networks receiving inputs from these directional selective neurons)? These directional selective neurons can be organised effectively and reliably for collision detection could suggest that similar organising strategies may be adopted in biological visual systems as well.

To answer the above question, this study will explore the properties of several possible postsynaptic organisations of these directional selective neurons for collision detection. Taking collision detection as the main visual task, we will explore the postsynaptic organisations of directional selective neurons via evolutionary processes. The evolved agents with the best postsynaptic structures will be challenged against challenging sequences, to examine the properties of these organisations. This investigation may not only bring new solution to road collision detection but also shed lights on further understanding of the possible postsynaptic neural structures of directional selective neurons in animals.

The rest of the paper is organised as follows: the mathematical formulation of the directional selective visual neurons is described in Section 2, the evolution algorithm setting, the fitness design and the evolving/testing environment are illustrated in Section 3, experiments and results are shown in Section 4, results and recent developments are further discussed in Section 5.

2. The vision system

The proposed vision system consists of two main parts. The first part is the whole field directional selective neurons [52,53] and their presynaptic network; different visual motion cues are extracted by this part of the vision system. The second part is the directional selective neurons' postsynaptic network (PN); the extracted visual motion cues are processed by this part of the vision system. Since the structures of the different directional selective neurons are similar, we choose a left inhibited directional selective neuron *L* [53] and a diagonally selective neuron *lu* (left-up) as examples to describe the directional selective neurons.

2.1. The directional selective neuron L and its presynaptic network

As an example, an *L* neuron, which responds to moving edges in all directions except the inhibited left direction, and its presynaptic network are illustrated (Fig. 1). The inhibition of the *L* neuron spreads in a unique way that it can cancel the left moving cues but leaving other moving cues unaffected. The network has four layers and one cell: a P layer, E/I layers, an S layer and an *L* neuron.

The first layer of the neural network is P layer. It consists of the photoreceptor *P* cells arranged in a matrix form; the luminance L_f of each pixel in the input image is captured by each photoreceptor cell, the change of luminance P_f between frames of the image sequence is calculated and forms the output of this layer. The output of a cell in this layer is defined by equation:

$$P_f(x,y) = |L_f(x,y) - L_{f-1}(x,y)| + \sum_{i}^{n_p} p_i P_{i-1}(x,y) \quad (1)$$

where $P_f(x,y)$ is the change of luminance at frame *f*, *x* and *y* are all in pixel, L_f and L_{f-1} are the luminance in current frame and in previous frame respectively, subscript *f* denotes the current frame and $f-1$ denotes the previous frame, the persistence coefficient p_i is varied from 0 to 1 with $p_i=(1+e^{\mu i})^{-1}$ and $\mu \in (-\infty, +\infty)$, n_p represents the maximum time steps the persistence can last.

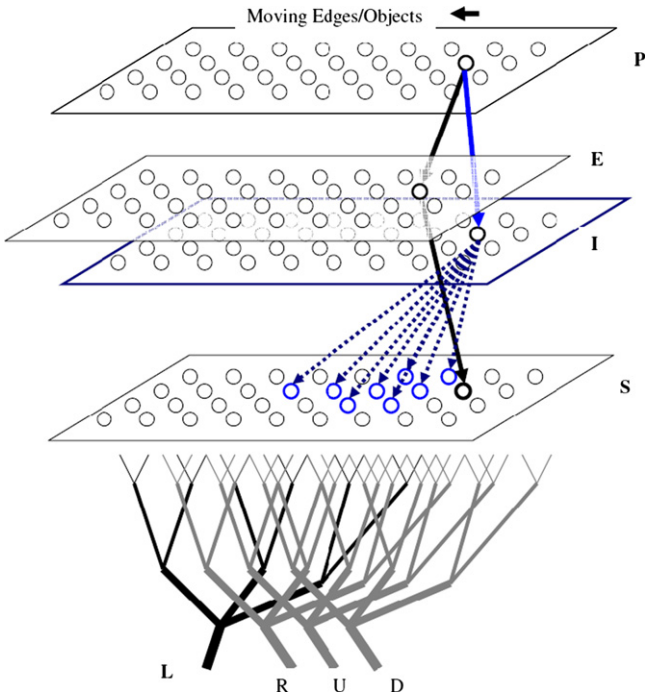

Fig. 1. A schematic illustration of a direction selective neuron L and its presynaptic neural network with the left side lateral inhibition. There are four groups of cells and one single cell in the system: photoreceptor cells (P); excitatory and inhibitory cells (E and I); summing cells (S); the left inhibited direction selective cell L. The lateral inhibition is indicated with dotted lines between I and S layer; the excitation is indicated with black lines between E and S layer. The connections between cells in P and E, P and I, E and S are one-to-one; only the connections to example cells are illustrated in this plot. The other direction selective cells, such as R, U and D, are with different inhibition preferences.

Cells in the E/I layers are arranged in matrix forms. The output of the *P* cells forms the two types of inputs to the cell in the E/I layers. One is excitation and the other is inhibition. The excitation of a *P* cell passes to its counterpart in the E layer and the inhibition from a *P* cell passes to its counterpart in the I layer directly.

Cells in the *S* layer are also arranged in a matrix form. The excitation of a *E* cell passes to its counterpart in the *S* layer directly. The inhibition from an *I* cell passes to its retinotopic counterpart's left side neighbouring cells in the S layer up to eight cells away with one image frame delay. The gathered strength of inhibition to a cell in this *S* layer is

$$I_f(x,y) = \sum_{i=1}^{n_{inh}} P_{f-1}(x+i,y) w_I(i) \quad (2)$$

where $I_f(x,y)$ is the inhibition to the cell in the *S* layer at (x, y), n_{inh} is the maximum number of cells in *I* layer that spread inhibition to the cell in the *S* layer at (x, y), $w_I(i) \in [0, 5.5]$ is the local inhibition weight which controls the neighbouring inhibition strength. With a strong inhibition (for example, $w_I(i)=5$) from the right side with one frame delay, the excitation caused by left moving edges can be eliminated or weakened sharply. The excitatory flow gathered in the *S* cell will be

$$E_f(x,y) = P_f(x,y) - I_f(x,y) W_I \quad (3)$$

where W_I is the global inhibition weight which control the overall inhibition strength.

The excitations exceed a threshold T_{rs} in the S cells are able to be summed by the left inhibitory cell L in the summing operation.

$$\tilde{E}_f(x,y) = \begin{cases} E_f(x,y), & if \quad E_f(x,y) \geq T_{rs} \\ 0, & if \quad E_f(x,y) < T_{rs} \end{cases} \tag{4}$$

The summed excitation of the left inhibitory cell L is,

$$Sum_f^L = \sum_{x=1}^{n_c} \sum_{y=1}^{n_r} |\tilde{E}_f(x,y)| \tag{5}$$

where n_r and n_c are the total number of cells in a row and a column in the S layer respectively. The summed excitation of the L cell is then sigmoid as,

$$s_f^L = (1+e^{-Sum_f n_{rc}^{-1}})^{-1} \tag{6}$$

where n_{rc} is the total number of the cells in the S layer. Since Sum_f^L is great than zero according to Eq. (5), the sigmoid excitation $s_f^L \in [0.5\text{–}1]$. Because the spatiotemporal processing mechanism described above, the left moving excitation will be eliminated or reduced by the left spreading inhibition within the L cell's presynaptic neural network. The L cell has one inhibitory direction, left, and is not expected to respond to left translating movements. The summed excitation of the L cell s_f^L is as one of the inputs to the following PNs.

Other directional selective neurons, for example the right directional selective neuron (R), the up directional selective neuron (U) and the down directional selective neuron (D) etc. share the same mechanism in forming their directional selectiveness. In Fig. 2, video sequence with a left running pedestrian is processed by the four different directional selective neurons, L, R, U and D simultaneously. The responded excitation of the directional selective neuron L is significantly different from that of the other three directional selective neurons as shown in the figure. Therefore, visual motion pattern in these images has been extracted by these directional selective neurons and can be used for further processing.

2.2. The diagonal directional selective neuron lu

Besides the above L, R, U and D directional selective neurons, other type of directional selective neurons which inhibit diagonal visual motion will also be used in this paper. These diagonal directional selective neurons are *lu* (left-up), *ld* (left-down), *ru* (right-up) and *rd* (right-down). The only difference between the diagonal directional selective neuron *lu* and the directional selective neuron L is the way inhibition is gathered by cells in S layer. For the *lu* cell, the inhibition from an I cell passes to its retinotopic counterpart's 'left-up' side neighbouring cells in the S layer up to eight cells away with one image frame delay. The Eq. (2), which describes the gathered strength of inhibition to a cell in this S layer, should be modified to describe the diagonal neuron lu,

$$I_f(x,y) = \sum_{i=1, i=j}^{n_{inh}} P_{f-1}(x+i, y-j) w_I(i,j) \tag{7}$$

For other diagonal directional selective neurons, the inhibition gathered by a cell in S layer can be illustrated in a similar way.

2.3. The postsynaptic networks

The schematic illustration of generic PNs is shown in Fig. 3(a). The inputs to the network are the excitation from the directional selective neurons, i.e.,

$$\{F\}_f^1 = (s_f^L s_f^R s_f^U s_f^D \cdots)^T \tag{8}$$

where s_f^L, s_f^R, s_f^U and s_f^D are the excitation in the L, R, U and D neurons, and $\{F\}_f^1$ is the input array to the PNs, f denotes frame number or time step. The output of the ith layer can be formulated in matrix form as:

$$\{F\}_f^i = [W]_f^i \{F\}_f^{i-1} \tag{9}$$

where $\{F\}_f^i$ and $\{F\}_f^{i-1}$ is the excitation array in ith and $i-1$th layer respectively, $[W]_f^i$ is the weight matrix.

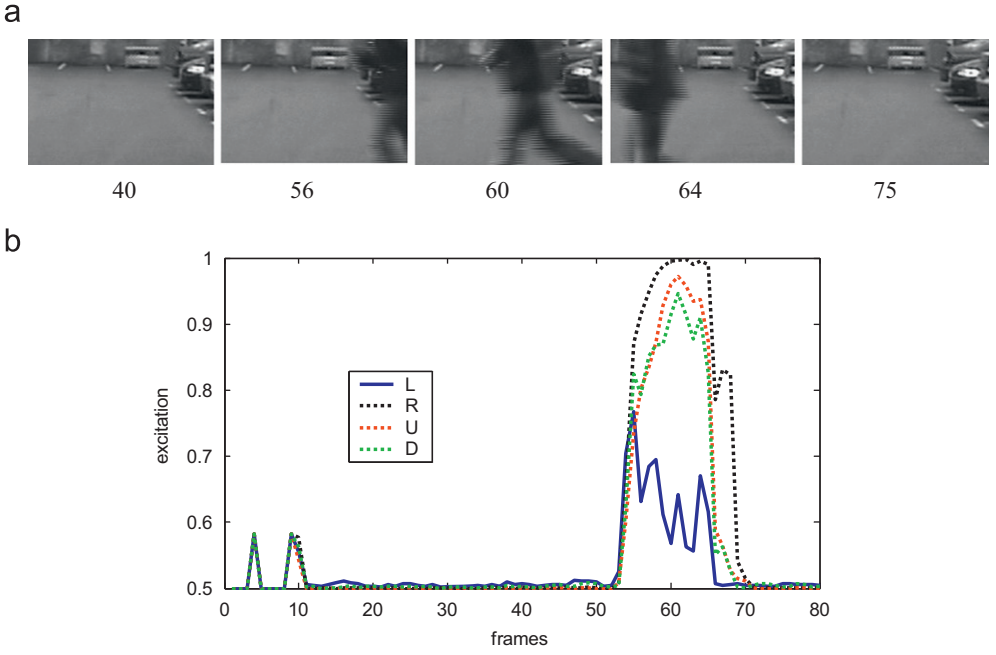

Fig. 2. An example of directional selective neurons process video sequences with a left running pedestrian. (a) sample images of the video sequences; the frame number is indicated under each image, (b) the excitation of the four Directional selective neurons: L (left), R (right), U (up) and D (down); note the left inhibited cell L's excitation is significantly lower than the other three directional selective neurons.

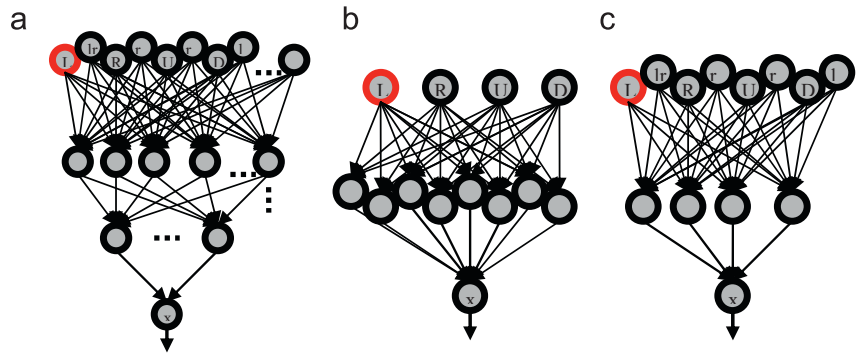

Fig. 3. Schematic illustration of PNs used in the study. (a) a generic multiple layered PN; it has number of directional selective neurons as input cells, layered intermediate cells and a spiking cell x as the output cell, (b) the dPN, with less (four) directional selective neurons as input cells, more (eight) intermediate cells and one spiking cell, (c) the vPN, with more (eight)) directional selective neurons as input cells, less (four) intermediate cells and one spiking cell.

The spiking cell x sums its adjacent layer's excitation. If the excitation κ_f in the spiking cell x exceeds the threshold T_{sp}, a spike is produced as the output,

$$S_f^{spike} = \begin{cases} 1 & f\ \kappa_f \geq T_{sp} \\ 0 & otherwise \end{cases} \tag{10}$$

where 1 represents a spike, 0 means no spike. A collision is predicted if there are n_{sp} spikes in n_{ts} time steps or frames ($n_{sp} \leq n_{ts}$), i.e.,

$$C_{coli} = \begin{cases} TRUE & if \sum_{f-n_{ts}}^{f} S_f^{spike} \geq n_{sp} \\ FALSE & otherwise \end{cases} \tag{11}$$

If C_{coli} turns to be *TRUE*, a collision is predicted by the neural vision system.

2.4. Parameters of the system

We assume that the development of the directional selective neurons has completed at this stage and the selectiveness of directional selective neurons is not the focus of this study. The coefficients in the directional selective neurons are treated as known variables in the evolution without change. Parameters in the directional selective neurons are set as following to ensure their directional selectiveness based on our experimental study. The persistence coefficient is set to be *0* to simplify the neural nets. The global inhibition weight W_I is set to be 1.5. The local inhibition weight $w_I(i)$ is set to be as strong as 5.5 to ensure inhibitory effect. The threshold in the *S* cells is set to be 12 based on trials. The directional selective neurons will be used in the experiments are: left inhibited neuron L, right inhibited neuron R, up inhibited neuron U, down inhibited neuron D, left-up diagonal inhibited neuron lu, left-down diagonal inhibited neuron ld, right-up diagonal inhibited neuron ru and right-down diagonal inhibited neuron rd. All the directional selective neurons used in this paper are set in the same way except the inhibited directions.

The connections and threshold within the PNs are adaptable in evolutions. However, as shown in Fig. 3(a), the possible internal connections and structural combination of these PNs are infinite. It is neither possible nor necessary to investigate all possible structured PNs. In this study, we take two typical PNs as representatives, as shown in Fig. 3(b) and (c). The two types of PNs differ clearly in the number of directional selective neurons in the input layer and the number of cells in hidden layers. The numbers of directional selective neurons and intermediate cells are identified important factors to the success of collision detections.

The two types of PNs (Fig. 3(b) and (c)), one with a big input layer and a small hidden layer (v-shaped PN, vPN hereafter), another with a small input layer and big hidden layer (diamond-shaped PN, dPN hereafter), are selected for the comparative evolutionary experiments. For each PN, connection weights are allowed to adapt between [−1.5 to 1.5] which is set empirically. The threshold of spiking cells is allowed to adapt within [0.0–10.0]. There are total 41 (for dPN) or 37 (for vPN) weights/thresholds are adaptable in the evolution. For all the PNs, five successive spikes indicate a collision has been predicted (i.e., $n_{sp}=n_{ts}=5$) by the vision system.

The scale of the vision system is associated with the size of input images. Since each pixel in an input image has one corresponding cell in the P layer of the PNs, there will be 8000 cells in the P layer suppose the input image is 100×80 pixels. The vision systems using a vPN has 8000 P cells, 8000 E cells and 8000 I cells all shared by its eight directional selective neurons; it has 64,000 S cells and 13 fusion cells; the total number of cells involved in the system is 88,013. Similarly, for the vision system using a dPN, the total number of cells in the system should be 56,013. At such a scale, the vision system with the vPN/dPN is able to process 100×80 pixels images at 30 frames per second on a DELL Precision 450 PC with a 2.5 GHz CPU.

3. Evolution of the vision system

Because there are many adaptable parameters in a PN as described above, a proper algorithm is needed to determine the weights/threshold to ensure the system achieves its best in road collision prediction. The search space of the neural vision system is typically complex, large and with little information on its structure. Evolutionary algorithm is particularly suitable for such tasks due to its efficiency in searching in a complex and large search space [17,18,13]. In this paper, evolutionary algorithms will be used to select the vision system. In the evolutions, the vision system will be represented by agents, which differ in connection weights/threshold. These agents are supposed to read the images, process them and output decisions autonomously.

3.1. Algorithm setting

A population of agents (30 hereafter, unless restated differently) in each generation are processed via evolutionary algorithms [8,51]. The first generation is produced randomly. To form a new generation, the worst performing agents (20% of the whole population in a generation) will be replaced. New agents (20% of a whole population) are produced by the best performing parents in the last generation through crossover. Mutation is conducted to

the chromosomes (binary coded) of these new produced agents with a mutation rate 0.2, which means to flip 20% of the randomly chosen binary bits in the chromosomes [51].

3.2. Fitness

Each agent's behaviour is evaluated based on its weighted success rate, i.e., fitness value. In each generation, an agent that responds to all visual events correctly, i.e. recognises imminent collisions and makes no false predictions on translating scenes or other challenges, scores a fitness value (success rate) of 100%; an agent that fails in all events scores a fitness value of 0%; an agent that fails in a non-colliding challenge scores a lowered fitness value (reduced success rate); an agent that fails in a colliding event gets a sharp reduction in success rate since a collision event is much more important in scoring than a non-collision one; for example, failure in a collision sequence may equal four times of failure in non-collision events. However, an agent scores 50% in fitness value if it only fails in all collision events or only fails in all no-collision events.

The fitness of an agent may be formulated as following:

$$F_k = \left(1 - \frac{\sum_{i=1}^{N_v} f_{event}^i}{M_{nb}}\right) \times 100\% \tag{12}$$

where F_k is the fitness value of the kth agent in the population, f_{event}^i is the score for the agent in ith events in the total N_v events, M_{nb} is the summation of all the possible scores, and f_{event}^i depends on performance: failure or success,

$$f_{event}^i = \begin{cases} K_{col} & \text{if fail in a collision event} \\ K_{non} & \text{if fail in a noncollision event} \\ 0 & \text{if success} \end{cases} \tag{13}$$

where K_{col} is the score for failure in a collision event, K_{non} is the score for failure in a non-collision event. For a collision event, failure means no collision signal has been sent out by the agent 3–30 frames before a real collision happens. K_{col} is several times bigger than K_{non} to assure an agent that only fails in all collision events and an agent that only fails in all non-collision events will have the same fitness value: 50%. In an evolutionary process, $N_v = 10$ (including 2 collision events), K_{col} is 4, K_{non} is 1 and M_{nb} is 16.

3.3. Evolving and testing environment

Driving environments and conditions may be very different in different places. Statistical data indicated that rear end collision is the most common accidents that involved two vehicles (e.g., [46,40]). Our vision system will focus on this type of collision. Driving scenes in which a car with a camera collides with another car will be selected as collision scenes. There are variety of non-collision scenes may cause false alarm, such as turning, changing lanes and in/out of tunnel etc, should also be included into the training and testing data bases. With the selected scenarios, we expect the evolved best vision agents should be able to recognise an impending collision and should not signal out false alarms to many other challenging but non-collision driving scenarios.

As illustrated in Fig. 4, a group of video sequences, which were originally recorded in real driving scenarios by our partner in Volvo Car Cooperation (Sweden), are selected to construct the environment. These video sequences are carefully selected from a video database consists of various driving scenes to represent typical challenging driving scenarios. Each sequence contains at least one event that causes strong excitation in the photoreceptor layer. These sequences include: collision with a car at about 30 and 60 mph, waiting and turning at a roundabout, walking and running pedestrians, road symbols, cutting in cars and high speed translating cars/vans. The car used for collision scene recording is an inflatable car for economical and safety reason. In these selected video clips, many of the frames are normal driving scenes without challenging visual motion. Since these video sequences were recorded with a camera fixed in a driving car, visual perturbations such as bumping and tilting were inevitable.

To select agents that are able to cope with collisions in different situations, an evolving environment may be expected

Fig. 4. Sample images from video footages represent a driving environment for the agents to evolve. The number under each image is the video sequence number. Video sequence 1 is a car collision scene while the agent is driving at a high speed, video sequence 2 is a car collision scene while the agent is driving at a low speed, video sequence 3 is a left translating van while the agent is waiting, video sequence 4 is a left running pedestrian while the agent is driving at very low speed, video sequence 5 is a left walking pedestrian while the agent is driving at very low speed, video sequence 6 is a turning car while the agent is driving at low speed, video sequence 7 is a fast translating car while the agent is waiting at a roundabout, video sequence 8 is a car cutting in while the agent is driving at normal speed on motor way, video sequence 9 is the scene with road symbols-arrow while the agent is driving at high speed, video sequence 10 is road symbols-arrows and zebra lines while the agent is driving down on the road at high speed.

to include as many visual events as possible. However, a huge video database may result in long or unacceptable training or evolving time. By carefully selecting visual events, the evolving environment described above should be able to cultivate agents coping with most of the visual challenges in road collision prediction. It should be stated that the vision system are targeting at big objects, such as cars and pedestrians in direct collision course. Because the presented vision system is based on visual motion processing, diversified events in terms of different objects, colour, texture and shape are not the essential factors in the evolving process. This is a distinct advantage of motion sensitive neuron based vision systems.

A group of sequences for testing the evolved agents are shown in Fig. 5(a). These test sequences include some of the challenging scenes in driving: the car with the recording camera is colliding with a car at about 45 mph; within its field of view, another car is doing translating movement at high speed; it is moving around a roundabout; it is approaching zebra crossing, pedestrians and driving in/out a tunnel. The best agents are expected to predict the collision in advance and should not signal out false alarm on other non-collision scenes.

Computer generated visual stimuli that are usually used by neurobiologist to challenge animals are also employed to check the consistency of the evolved agents (Fig. 5(b)). These visual stimuli (Fig. 5(b)) contain only generalised motion cues, such as expanding edges and translating cues, and have avoided environmental bias resulted from complex visual scenes.

All the input sequential images fed to the visual collision detection system are resized to 100 (in horizontal) times 80 (in vertical) pixels; images are transformed from colour to grey ranging from 0 to 255. As mentioned earlier, the original video sequences were all taken at 25 frames per second (fps) directly in driving scenarios. These video sequences have all been resized and transformed to grey level video sequences with a resolution of 100×80 pixels and grey level of 0–255 before the experiments.

4. Experiments and results

In our experiments, each evolution process usually lasted about 13–14 hours with a population of 30 individuals, 20% generation refresh rate and 400 generations on a Dell Precision 450 PC with 2.50 GHz CPU. Before the evolving experiments, it has been tested that each agent was able to work at 30 image frames per second run in the same PC with 2.50 GHz CPU. The long hours of evolution process is coming from the huge image processing needs: 400 generations, each generation has 30 individuals with 20% new generated individual, each new individual has to process all the video clips that contains several hundreds of frames—this takes time even at a rate of 30 frames per second.

The two groups of agents, with dPN or vPN in their vision system, evolved for 400 generations respectively in the driving environment. For each of the group, evolution processes have been carried out and repeated for three times. The best agents were then tested with new test driving sequences as sampled in Fig. 5(a). Results are shown in Figs. 6–9 and Table 1. The properties of the best agents were also further checked by challenging them with visual stimuli used by neurobiologist to challenge animals, as shown in Fig. 5(b).

In Fig. 6, the fitness value (or success rate) of the best agents from each generation in each round of evolution and the mean

Fig. 5. (a) Sample images of the test sequences. Video sequence 1 is a car collision at normal speed (about 60 mph), video sequence 2 is a right translating car while the agent is turning around roundabout, video sequence 3 is pedestrians and zebra lines while the agent is driving slowly, video sequence 4 is a translating car and road lines while turning at high speed, video sequence 5 is zebra lines while the agent is driving at ordinary speed, video sequence 6 is a right translating car while the agent is waiting signal, video sequence 7 is a left translating car while the agent is waiting signal, video sequence 8 is a pedestrian with trolley while the agent is driving slowly, video sequence 9 is a tunnel while the agent is driving at cruising speed, video sequence 10 is a right turn, video 11 is a pedestrian walking from right to left while the agent is driving slowly, video sequence 12 the agent is driving after a truck, video sequence 13 is the agent driving slowly in a supermarket area where customers were pushing trolley around, video sequence 14 is a normal driving scene with cars and truck ahead and video sequence 15 is the agent driving slowly while a pedestrian was walking quickly in front of the car. (b) Computer generated visual stimuli with a 100×80 pixels field of view. Left: black square (10 pixels times 10 pixels originally) expands to 60×60 pixels with an expanding rate of 5 and 10 pixels per frame respectively; middle: black bar (15 pixels times 40 pixels) with a translating speed at 6 and 12 pixels per frame to left respectively; right: black bar (15 pixels times 40 pixels) with a translating speed at 6 and 12 pixels per frame to right respectively. The arrows are added for schematically indicating visual stimuli moving directions.

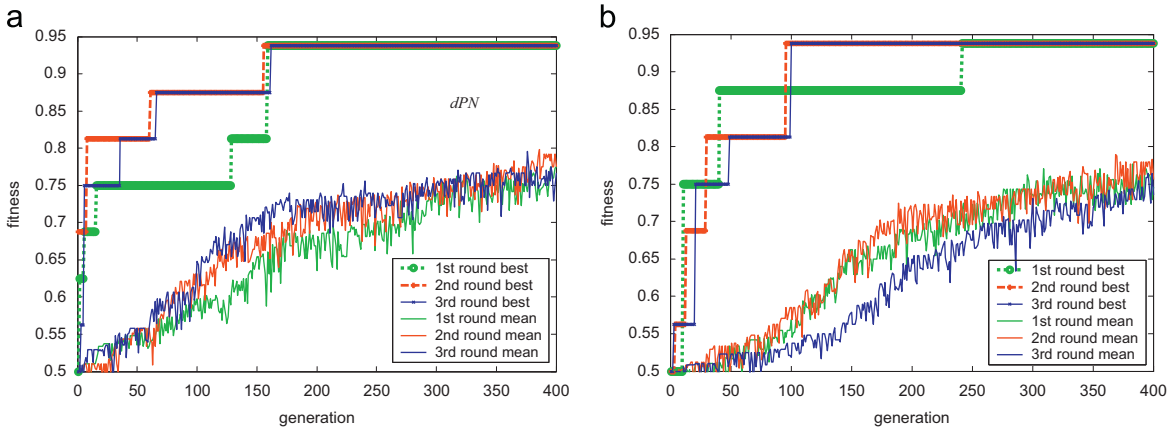

Fig. 6. The fitness versus generation. The best fitness is the best agent's fitness value in each round of evolution. The mean fitness is the averaged fitness value of a whole population in a generation in each round of evolution. Evolutions are conducted in three separate rounds for each type of agent. (a) the evolution results of the dPN; (b) the evolution results of the vPN.

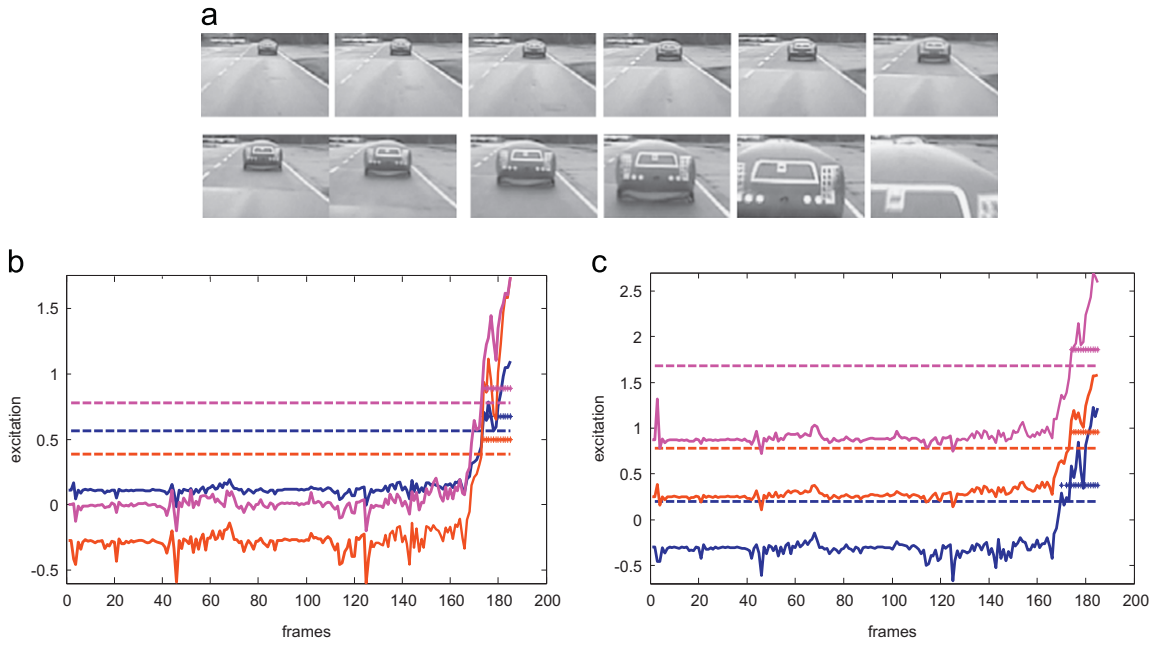

Fig. 7. The excitation of the spiking cell x of the best agents in processing the collision event (Fig. 4, sequence 1). The three agents used in comparison are picked up from the three separated evolutions respectively. The collision happened at frame 195. The six agents are all capable of detecting the collision properly. The excitations are in solid lines. The thresholds are indicated with dashed lines. Decisions are made by five successive spikes indicated by five asterisks. The lines and asterisks with the same colour are belonging to the same agent. (a), from top left to bottom right sample images at 80, 90, … till 190 at every 10 frames, (b) agents with dPN, (c) agents with vPN.

fitness value averaged from each generation in each round of the evolution were shown respectively. The best agents started with very low success rates—around 50%. By the 400th generation all the best agents can predict imminent collisions with high success rate (94%), despite different PNs in the vision system. Six best performed agents are selected from each evolution process and their performances are detailed in Table 1. All the six agents can detect collisions correctly and can cope with most of the non-collision scenes properly; however, all six failed in the same challenge: driving down approaching pedestrian crossing lines at high speed (Table 1 and Fig. 4, video sequence 10).

The properties detailed excitation level of the spiking cells of the six best agents, when challenged with a colliding car (Fig. 4, no. 1), a translating pedestrian (Fig. 4, no. 4) and zebra lines (Fig. 4, no. 10) are shown in Figs. 7 and 8. It is found that the six spiking cells respond to collision similarly with high excitation and successive spikes (Fig. 7), though the absolute excitation value in each agent is different. Interestingly the responses of these agents to the pedestrians are quite different: some with higher level of excitation and sparse spikes; some with lower level of excitation and no spike; however, neither detected it as a collision scene, i.e. did not produce successive spikes (Fig. 8).

To see if the evolved best agents perform similarly in similar situations, these six best agents are then challenged with test sequences (Fig. 5(a)). Results are shown in Table 2. There are three agents (two with dPN and one with vPN) passed the entire test with very high success rate. These agents detected the collision about 15–19 frames ahead of real collision, leaving 600–760 ms to deploy measures to avoid or mitigate the impact of the collision. Compare to the agent with a special structured PN [53], the best evolved agents detected the collision about 9–13 image frames (i.e., 360–520 ms) earlier which implies higher probability to avoid or reduce the impact of the collision. There are three best agents failed in the high speed turning scenario (Fig. 5(a), no. 4), two of which are with the vPN. As to the zebra crossing, only one agent sent out a false collision alarm, the others all performing correctly.

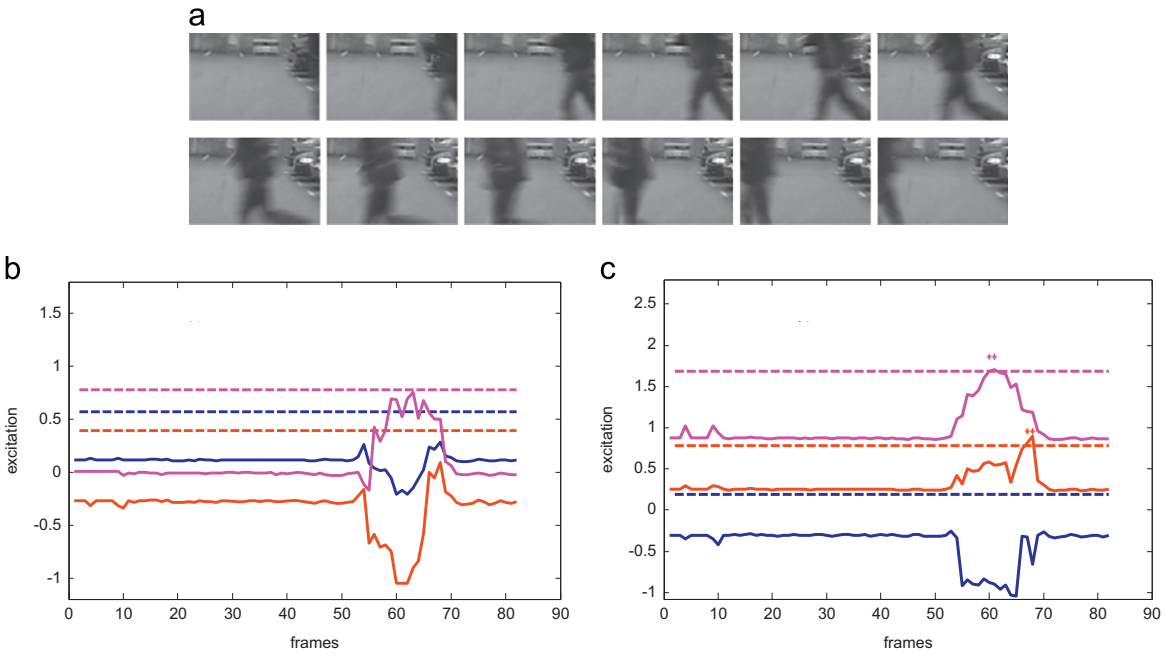

Fig. 8. The excitation of the spiking cell x of the best agents in processing the fast translating events (Fig. 4, sequence 5). The six agents used in comparison are picked up from the six separated evolutions respectively. The six evolved best agents are all capable of dealing with the fast translating events correctly without sending out false alarm. The excitations are in solid lines. The thresholds are indicated with dashed lines. The lines and asterisks with the same colour are belonging to the same agent. Collision decisions may be made by five successive spikes indicated by five asterisks. (a) from top left to bottom right sample images at 55, 56, … till 66 at every 1 frame, (b) agents with dPN, (c) agents with vPN.

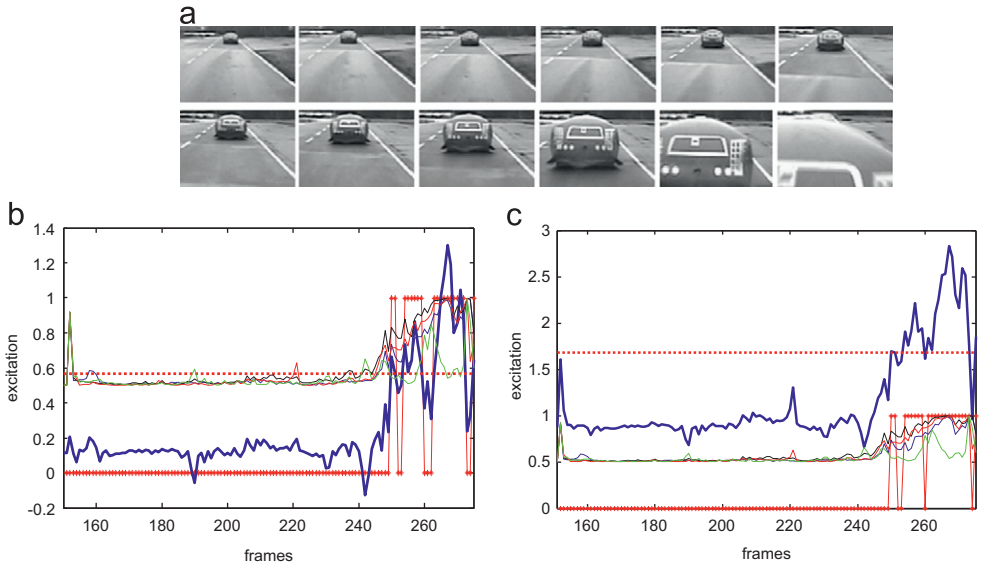

Fig. 9. The best agents challenged with test driving sequences when the car with the camera collides with a balloon car. The best agent with dPN is from the 1st round of evolution. The best agent with vPN is from the 3rd round of evolution. The threshold is indicated in doted horizontal lines; spikes are indicated with up asterisks; the excitation is plotted in solid lines. The excitations of the L, R, U and D cells are in blue, black, red and green respectively (hereafter in other figures). (a) from top left to bottom right sample images at 160, 170, … till 270 at every 10 frames; real collision happened at frame 273, (b) the response of the best agent with dPN; the collision is predicted at frame 258, (c) the response of the best agent with vPN; the collision is predicted at frame 258.

To demonstrate the properties of these evolved postsynaptic organisations, the detailed responses of two selected best agents-one with dPN and the other with vPN to car collision (Fig. 5(a), no.1), pedestrians (Fig. 5(a), no. 3), and tunnel (Fig. 5 (a), no. 9) are shown in Figs. 9, 10 and 11 respectively. The best agent with dPN is from the 1st round of evolution and the best agent with vPN is from the 3rd round of evolution. Both of the agents predicted the collision early at frame 258 (Fig. 9) as also indicated in Table 2. To the challenging scene of driving into tunnel, both agents responded with very low level of excitation, as shown in Fig. 10. This means the best agents were able to distinguish the difference between the tunnel and the colliding car. Because of the size of a tunnel, its expanding pattern is different to that of a car. As to pedestrians, the two best agents responded with low excitation (Fig. 11). It is noted that, as the car was driving slowly approaching the pedestrians (means the images of these pedestrians and zebra lines were expanding slowly), the excitation levels of the two agents actually climbed up and remained high between frame 160–210 as shown in the figure.

The above test demonstrated the ability of the best evolved agents in detecting car collision while maintaining low level of

Table 1
The performance of the six best agents with vPN or dPN after evolution.

Evolution	Performance of the six best evolved agents					
Sequences	dPN			vPN		
	1	2	3	1	2	3
1 (195)	√(183)	√(178)	√(178)	√(176)	√(178)	√(178)
2 (124)	√(117)	√(108)	√(108)	√(108)	√(108)	√(108)
3	√	√	√	√	√	√
4	√	√	√	√	√	√
5	√	√	√	√	√	√
6	√	√	√	√	√	√
7	√	√	√	√	√	√
8	√	√	√	√	√	√
9	√	√	√	√	√	√
10	×(100)	×(95)	×(97)	×(93)	×(96)	×(96)
Fitness (%)	94	94	94	94	94	94

Note: √ indicates an agent responds to that event correctly; × indicates an agent fails in that event. Only sequence no.1 is the collision sequence. The number in brackets after each sequence number is the frame at which a real collision happens; the number in brackets after each performance marker (√ or ×) is the frame at which a collision is predicted by the best agent. The fitness equals to success rate.

Table 2
The performance of the six best agents with vPN and dPN challenged with the TEST sequences.

TEST	Performance of the six best agents					
Sequences	dPN			vPN		
	1	2	3	1	2	3
1(273)	√(258)	√(254)	√(257)	√(254)	√(254)	√(258)
2	√	√	√	√	√	√
3	√	√	√	√	√	√
4	√	√	×(438)	×(438)	×(438)	√
5	√	√	√	×(190)	√	√
6	√	√	√	√	√	√
7	√	√	√	√	√	√
8	√	√	√	√	√	√
9	√	√	√	√	√	√
10	√	√	√	√	√	√
11	√	√	√	√	√	√
12	√	√	√	√	√	√
13	√	√	√	√	√	√
14	√	√	√	√	√	√
15	√	√	√	√	√	√

Note: √ indicates an agent responds to that event correctly; × indicates an agent fails in that event. Only sequence no.1 is the collision sequence. The number in brackets after each sequence number is the frame at which a real collision happens; the number in brackets after each performance marker (√ or ×) is the frame at which a collision is predicted by the best agent.

false alarm. The results may also suggest that four directional selective neurons are probably enough for collision detection because the best dPN agent can deal with these sequences very well and the best vPN agents with more directional selective neurons have not been able to show better performance in these experiments.

In other evolution experiments, we have also organised directional selective neurons with other types of layered PNs; for example, PNs with different number of cells in hidden layer, PNs with multiple hidden layers. The highest fitness of the agents with these PNs also reached 94%. With these PNs, the best agents only fail in the zebra crossing scene (Fig. 5(a), video sequence 10), exactly the same as dPN and vPN agents did. However, the fitness of best agents can only reach 88% if the number of directional selective neurons is reduced to two. This may indicate that only considering visual motion in two dimensions is not sufficient for a road collision detection system.

Although the best agents are expected to compare and/or combine the extracted visual cues—the expanding/moving edges of objects for collision detection, there is concern about the real working pattern of these evolved best agents. Since only two collision events were included in the evolving environment, the best agents may pick up special visual cues instead of the expanding/moving edges to make up their decisions. To further investigate the working pattern of the agents, two of the best evolved agents with different PNs were then challenged with computer generated visual stimuli which are similar to those used by neurobiologists to challenge animals (Fig. 5(b)). Results are shown in Fig. 12(a) and (b) respectively. Both of the best agents have shown the ability to distinguish a looming stimulus from translating ones with different excitation patterns. The best agents responded to the looming square with constant high level excitation; for the translating bars, they responded with peaked excitation, then lower level excitation and finished with another sharp valley. Different visual motion speed had not affected these patterns very much, as shown in Fig. 12. These results were consistent with the previous founding in the driving experiments and demonstrated the robustness of this pattern recognition mechanism.

5. Further discussion

In the above sections, evolution processes have been conducted to further explore the postsynaptic networks of directional motion sensitive neurons by selecting best evolved vision agents for collision scene recognition. The experiments demonstrated that the proposed vision system can be evolved to detect collision earlier compare to special structured postsynaptic network [53]. The experimental results suggested that, the proposed PNs are among the very competent postsynaptic networks that fuse the outputs of directional selective neurons efficiently and reliably for collision detection.

Directional selective neurons have been identified in many normally functioning visual system studied, (for example, in insects [16,33,34,7]; in vertebrates [2,3,44,47,12,32,24]). The mechanisms underlying directional selective neurons in animal are still under investigation. The interaction of these directional selective neurons to guide behaviours in animals is also a subject of speculation. The interactions of different visual interneurons in insects are complex, (for example, [45,23]). Modelling studies have provided chances to investigate possible mechanisms for information processing postsynaptically connected to these neurons for specific visual tasks, such as collision detection. The results revealed above, together with the finding in [53], may suggest that it is plausible for directional selective neurons in animals to be involved in collision avoidance.

The presented bio-inspired vision system recognises road collision scenes based on visual motion cues extracted by directional selective neurons. One distinct feature of a motion sensitive vision system is that it processes differential images which are irrelevant or less relevant to the shapes, colours and textures of colliding objects and background movements. Compared to other segmentation/registration based computer vision methods that have to spend huge computing cost on shapes, colours and textures, the proposed vision system can operate at high frame rate (30 fps) due to its low computing power consumption.

As mentioned earlier, the presented vision system focused on rear end car collision. The evolving environment which consisted of the ten selected video sequences only represented a small fraction of the many types of road collisions happened in real

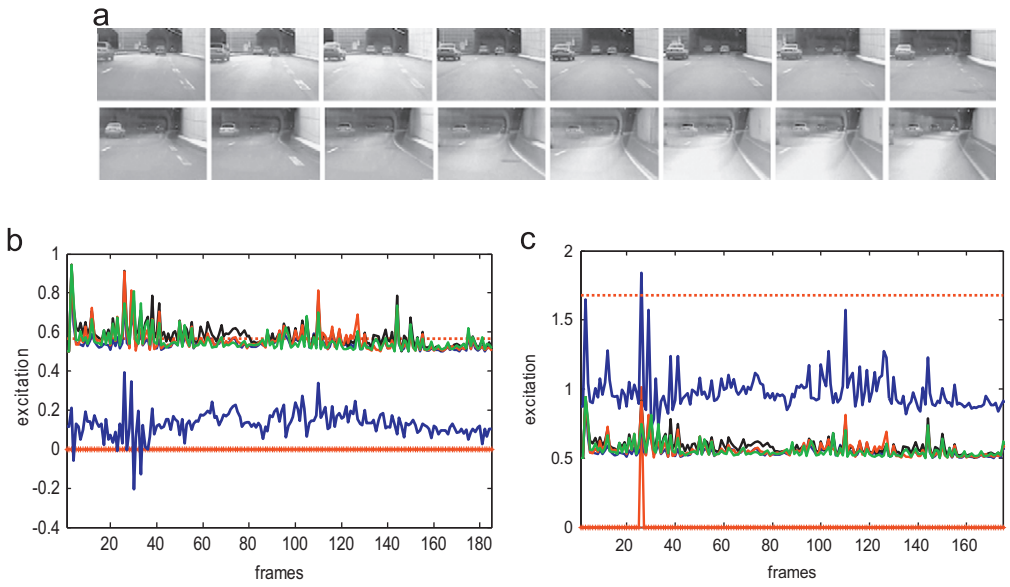

Fig. 10. The best agents challenged with test driving sequences when the car with the camera get into a tunnel. The best agent with dPN is from the 1st round of evolution. The best agent with vPN is from the 3rd round of evolution. The threshold is indicated in doted horizontal lines; spikes are indicated with up asterisks; the excitation is plotted in thick solid lines. (a) from top left to bottom right sample images at 20, 30, … till 170 at every 10 frames, (b) the response of the best agent with dPN; no collision is predicted, (c) the response of the best agent with vPN; no collision is predicted.

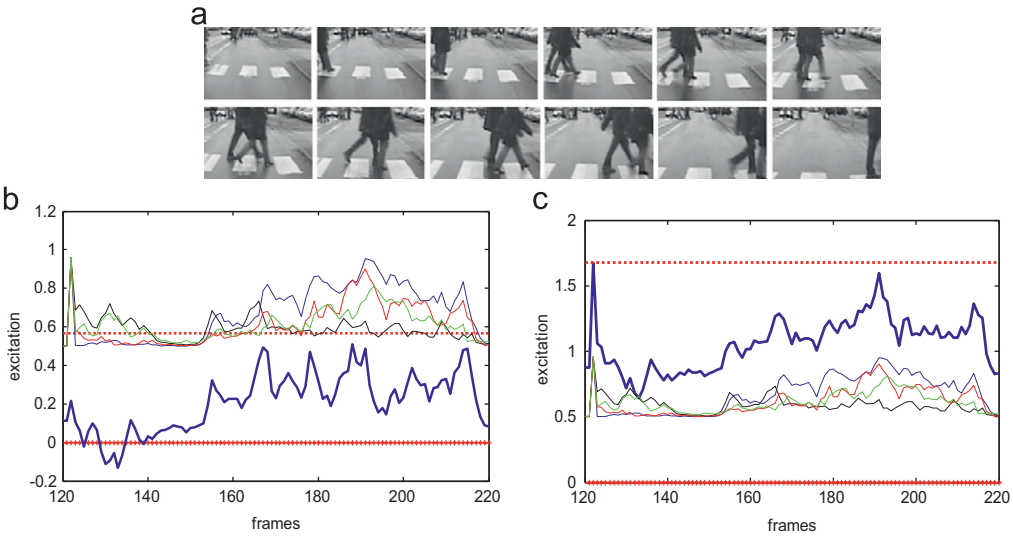

Fig. 11. The best agents challenged with test driving sequences when the car with the camera was driving slowly towards the pedestrians on zebra crossing. The best agent with dPN is from the 1st round of evolution. The best agent with vPN is from the 3rd round of evolution. The threshold is indicated in doted horizontal lines; spikes are indicated with up asterisks; the excitation is plotted in solid lines. (a) from top left to bottom right sample images at 155, 160… till 210 at every 5 frames, (b) the response of the best agent with dPN; no collision is predicted, (c) the response of the best agent with vPN; no collision is predicted.

world. Many other road collisions, for example collision with pedestrian(s), were not included in the evolving and testing databases because these collision video footages were proved to be hard for us to make due to safety and economic reasons. In the future, we may use computer simulated video sequences once the quality of these sequences reach to an acceptable level.

The fast processing speed of these bio-inspired algorithms, which have easily reached to 30 frames per second in the PC, can be further accelerated dramatically when integrated further with or realized in suitable hardware. For example, the LGMD neural network can reach above 60 frames per second when implemented in a FPGA [27]. It is also predictable that, even using a PC, the processing speed of the collision detection system can be further accelerated if most of the image processing task can be assigned to an integrated GPU. The powerful parallel processing ability of these bio-inspired visual processing algorithms can be achieved eventually if, in the future, being designed and realized in VLSI chips.

There are more than 100 inter-neurons in a locusts' lobula plate working simultaneously allowing it interacts with dynamic environments smartly. Though directional selective neurons-based network can recognise collisions among many confusing scenes, it is obvious that only directional selective neurons and its postsynaptic network alone are not enough to detect many types of collision scenes. Other specialized neural systems, such as LGMD [49,50], should also be integrated into the vision system to deal with diversified collision patterns.

In future, the coordination between the presented directional selective neurons based vision system and the LGMD-based vision system for collision detection will be investigated systematically via co-evolutionary process. Methods that allow the structure of

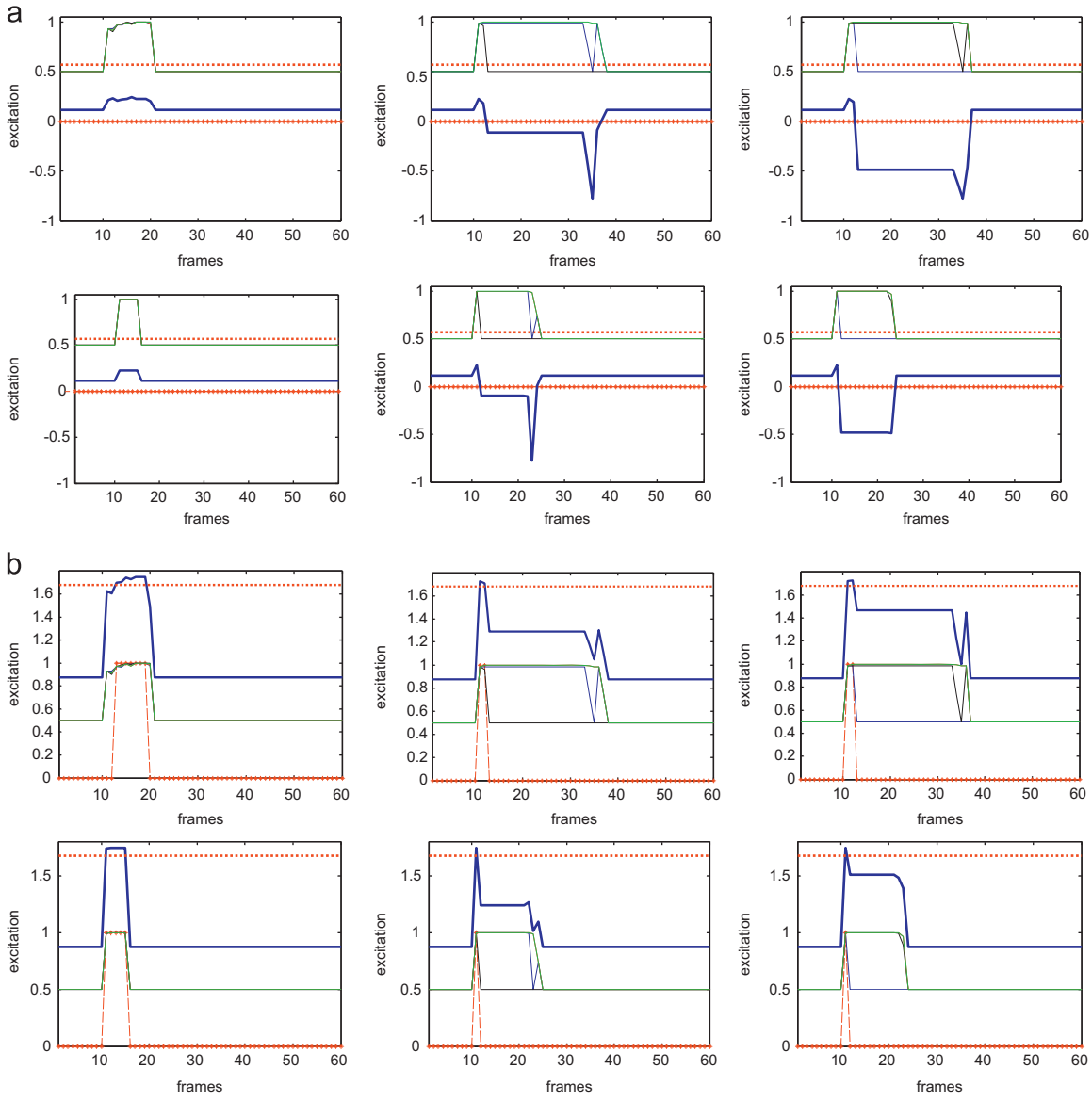

Fig. 12. The excitation level of the two best agents when processing computer generated visual stimuli. The excitation is plotted in solid bold lines; other symbols are the same as Fig. 12. Left column shows the excitation level of x cell of the agents when they were challenged with a computer generated looming square (Fig. 5(b), left) with expanding rates at 5 pixel per frame (1st and 3rd row) and 10 pixel per frame (2nd and 4th row) respectively; central column shows the excitation when the agents were challenged with a translating bar (Fig. 5(b), middle), at 6 pixel per frame (1st and 3rd row) and 12 pixel per frame (2nd and 4th row) to left respectively; right column shows the excitation when the agents were challenged with a translating bar to the left (Fig. 5(b), right) at 6 pixel per frame (1st and 3rd row) and 12 pixel per frame (2nd and 4th row) respectively. (a) The best agent is with dPN selected from the first round of evolution. (b) The best agent is with vPN selected from the third round of evolution.

PN to evolve will also be investigated. Since the bio-inspired image processing system achieves its current performance by regulating excitation and inhibition spatiotemporally via layered structures, these unique computing structures can be realized to VLSI chips and mass produced for different applications.

6. Conclusions

In the above sections, we further investigated postsynaptic organisations of specialized visual motion sensitive neurons—whole field directional selective neurons for collision detection in a driving environment. Inspired by biological vision systems, directional selective neurons can extract different directional visual motion cues reliably by allowing inhibition spreads to further layers in specific directions with time delay. As postsynaptic organisations of directional selective neurons, different PNs have been evolved and selected through evolutionary processes and the evolved best agents have then been tested with challenging test video sequences. The results of our experiments showed that the best agents are able to predict impending collisions reliably while avoiding disturbances from other non-collision events. This study demonstrated that whole field directional selective neurons are able to be organised efficiently by those proposed postsynaptic neural networks for collision detection in complex visual environments. The results suggested that the presented vision systems are among the candidates to be realized in vision-chips for collision detection.

Acknowledgement

This research was partly supported by EU FP7-IRSES projects EYE2E (269118) and LIVCODE (295151). We thank Mr. Martti Soininen of Volvo Car Corporation for providing the driving video

sequences used in this paper. We thank the anonymous reviewers for their valuable comments and suggestions on the 1st and 2nd revision of the manuscript.

References

[1] A. Amditis, A. Polychronopoulos, N. Floudas, L. Andreone, Fusion of infrared vision and radar for estimating the lateral dynamics of obstacles, Inf. Fusion 6 (2005) 129–141.
[2] H.B. Barlow, R.M. Hill, Selective sensitivity to direction of movement in ganglion cells of rabbit retina, Science 139 (1963) 412–414.
[3] H.B. Barlow, W.R. Levick, Mechanism of directionally selective units in rabbits retina, J. Physiol. 178 (1965) 477–504.
[4] V. Belevskiy, S. Yue, Near range pedestrian collision detection using bio-inspired visual neural networks, in: Proceeding of the International Conference on Natural Computation, Shanghai, China, 26–29 July, 2011, pp. 786–790. Digital Object Identifier: Doi: 10.1109/ICNC.2011.6022169.
[5] M. Blanchard, P.F.M.J. Verschure, F.C. Rind, Using a mobile robot to study locust collision avoidance responses, Int. J. Neural Syst. 9 (1999) 405–410.
[6] M. Blanchard, F.C. Rind, P.F.M.J. Verschure, Collision avoidance using a model of the locust LGMD neuron, Robotics and Autonomous Syst. 30 (2000) 17–38.
[7] A. Borst, J. Haag, Neural networks in the cockpit of the fly, J. Comp. Physiol. 188 (2002) 419–437.
[8] A.J. Chipperfield, P.J. Fleming, The Matlab genetic algorithm toolbox, in: Proceedings of the IEE Colloquium on Applied Control Techniques Using MATLAB, Digest No.1995/014, 26 January 1995.
[9] J.D. Davis, S.F. Barrett, C.H. Wright, M. Wilcox, A bio-inspired apposition compound eye machine vision sensor system, Bioinspir. Biomim. 4 (4) (2009) 0046002.
[10] G.N. DeSouza, A.C. Kak, Vision for mobile robot navigation: a survey, IEEE Trans. Pattern Anal. Mach. Intelli. 24 (2) (2002) 237–267.
[11] N. Franceschini, Visual guidance based on optic flow: a biorobotic approach, J. Physiol. Paris 98 (2004) 281–292.
[12] S.I. Fried, T.A. Muench, F.S. Werblin, Mechanisms and circuitry underlying direction selectivity in the retina, Nature 420 (2002) 411–414.
[13] D.E. Goldenberg, Genetic Algorithms in Search, Optimization and Machine Learning, Addison-Wesley, Reading, Massachusetts, 1989.
[14] E. Guizzo, How Google's self-driving car works, IEEE Spectrum, Robotics Blog 18 (2011).
[15] R.R. Harrison, C. Koch, A silicon implementation of the fly's optomotor control system, Neural Comput. 12 (2000) 2291–2304.
[16] B. Hassenstein, W. Reichardt, Systemtheorische analyse der Zeit-, Reihenfolgen- und Vorzeichenauswertung bei der Bewegungsperzeption des Rüsselkäfers Chlorophanus, Zeitschrift für Naturforschung 11b (1956) 513–524.
[17] J.H. Holland, Adaptation in Natural and Artificial Systems, The University of Michigan Press, Ann Arbor, 1975.
[18] J.H. Holland, ECHO: explorations of evolution in a miniature world, J.D. Farmer, J. Doyne (eds.), in: Proceedings of the Second Conference on Artificial Life, Addison-Wesley, 1990.
[19] G.A. Horridge, What can engineers learn from insect vision? Phil. Trans. R. Soc. Lond. 337 (1992) 271–282.
[20] S.A. Hubber, M.O. Franz, H.H. Buelthoff, On robots and flies: modelling the visual orientation behaviour of flies, Robotics Autonomous Syst. 29 (1999) 227–242.
[21] F. Iida, Biologically inspired visual odometer for navigation of a flying robot, Robotics Autonomous Syst. 44/3–44/4 (2003) 201–208.
[22] G. Indiveri, R. Douglas, Neuro-vision sensors, Science 288 (2000) 1189–1190.
[23] H.G. Krapp, B. Hengstenberg, R. Hengstenbeg, Dendritic structure and receptive-field organization of optic flow processing interneurons in the fly, J. Neurophysiol. 79 (4) (1998) 1902–1917.
[24] M.S. Livingstone, Direction inhibition: a new slant on an old question, Neuron 45 (2005) 5–7.
[25] M.S. Lee, Y.H. Kim, Automotive radar tracking of multi-target for vehicle CW/CA systems, Mechatronics 14 (2004) 143–151.
[26] R. Manduchi, A. Castano, A. Talukder, L. Matthies, Obstacle detection and terrain classification for autonomous off-road navigation, Autonomous Robots 18 (2005) 81–102.
[27] H. Meng, K. Appiah, S. Yue, A. Hunter, M. Hobden, N. Priestley, P. Hobden, C. Pettit, A modified model for the lobula giant movement detector and its FPGA implementation, Comput. Vis. Image Understanding 114 (18) (2010) 1238–1247.
[28] L. Muratet, S. Doncieux, Y. Briere, J.A. Meyer, A contribution to vision-based autonomous helicopter flight in urban environments, Robotics Autonomous Syst. 50 (2005) 195–209.
[29] A. Najmi, A. Mahrane, D. Esteve, G. Vialaret, J.J. Simonne, Pulsed LIDAR for obstacle detection in the automotive field: the measurement of reflectance range data in scene analysis, Sensors and Actuators, A 46–47 (1995) 497–500.
[30] M. O'Shea, C.H.F. Rowell, J.L.D. Williams, The anatomy of a locust visual interneuron: the descending contralateral movement detector, J. Exp. Biol. 60 (1974) 1–12.
[31] C. Pan, H. Deng, X.F. Yin, J.G. Liu, An optical flow-based integrated navigation system inspired by insect vision, Biol. Cybern. 105 (3–4) (2011) 239–252.
[32] N.J. Priebe, D. Ferster, Direction selectivity of excitation and inhibition in simple cells of the cat primary visual cortex, Neuron 45 (2005) 133–145.
[33] F.C. Rind, A directionally selective motion-detecting neurone in the brain of the locust: physiological and morphological characterization, J. Exp. Biol. 149 (1990) 1–19.
[34] F.C. Rind, Identification of directionally selective motion-detecting neurones in the locust lobula and their synaptic connections with an identified descending neurone, J. Exp. Biol. 149 (1990) 21–43.
[35] F.C. Rind, P.J. Simmons, Orthopteran DCMD neuron: A re-evaluation of responses to moving objects. I. Selective responses to approaching objects, J. Neurophysiol. 68 (1992) 1654–1666.
[36] F.C. Rind, D.I. Bramwell, Neural network based on the input organization of an identified neuron signalling impending collision, J. Neurophysiol. 075 (1996) 967–985.
[37] F.C. Rind, P.J. Simmons, Seeing what is coming: building collision sensitive neurons, Trends Neurosci. 22 (1999) 215–220.
[38] F.C. Rind, Motion detectors in the locust visual system: from biology to robot sensors, Microsc. Res. Tech. 56 (2002) 256–269.
[39] F.C. Rind, Roger D. Santer, J.Mark Blanchard, Paul F.M.J. Verschure, Locust's looming detectors for robot sensors, in: F.G. Barth, J.A.C. Humphrey, T.W. Secomb (Eds.), Sensors and Sensing in Biology and Engineering, Spinger-Verlag, Wien, New York, 2003.
[40] Road casualties Great Britain, 2006. Annual Report, 〈http://www.dft.gov.uk〉.
[41] R.D. Santer, R. Stafford, F.C. Rind, Retinally-generated saccadic suppression of a locust looming detector neuron: investigations using a robot locust, J. R. Soc. Lond. Interface 1 (2004) 61–77.
[42] G.R. Schlotterer, Response of the locust descending contralateral movement detector neuron to rapidly approaching and withdrawing visual stimuli, Can. J. Zool. 55 (1977) 1372–1376.
[43] R. Stafford, R.D. Santer, F.C. Rind, A bio-inspired visual collision detection mechanism for cars: combining insect inspired neurons to create a robust system, Biosystems 87 (2007) 162–169.
[44] S.F. Stasheff, R.H. Masland, Functional inhibition in direction-selective retinal ganglion cells: spatiotemporal extent and intralaminar interactions, J. Neurophysiol. 88 (2002) 1026–1039.
[45] L.F. Tammero, M.H. Dickinson, Collision-avoidance and landing responses are mediated by separate pathways in the fruit fly, *Dorsophila melanogaster*, J. Exp. Biol. 205 (18) (2002) 2785–2798.
[46] A. Vahidi, A. Eskandarian, Research advances in intelligent collision avoidance and adaptive cruise control, IEEE Trans. Intell. Transp. Syst. 4 (3) (2003) 143–153.
[47] D.I. Vaney, W.R. Taylor, Direction selectivity in the retina, Curr. Opinion Neurobiol. 12 (2002) 405–410.
[48] B. Webb, R. Reeve, Reafferent or redundant: integration of phototaxis and optomotor behaviour in crickets and robots, Adaptive Behav. 11 (3) (2003) 137–158.
[49] S. Yue, F.C. Rind, A collision detection system for a mobile robot inspired by locust visual system, in: Proceedings of the IEEE International Conference on Robotics and Automation, Spain, Barcelona, April18–21, 2005, pp. 3843–3848.
[50] S. Yue, F.C. Rind, Collision detection in complex dynamic scenes using a LGMD based visual neural network with feature enhancement, IEEE Trans. Neural Networks 17 (3) (2006) 705–716.
[51] S. Yue, F.C. Rind, M.S. Keil, J. Cuadri, R. Stafford, A bio-inspired visual collision detection mechanism for cars: optimisation of a model of a locust neuron to a novel environment, Neurocomputing 69 (13–15) (2006) 1591–1598.
[52] S. Yue, F.C. Rind, Visual motion pattern extraction and fusion for collision detection in complex dynamic scenes, Comput. Visi. Image Understanding 104 (1) (2006) 48–60.
[53] S. Yue, F.C. Rind, A synthetic vision system using directional selective motion detectors for collision recognition, Artif. Life 13 (2) (2007) 93–122.
[54] S. Yue, F.C. Rind, Near range path navigation using LGMD visual neural networks, in: Proceedings of the International Conference on Artificial Intelligence and Neural Networks, Beijing, August 2009, pp. 105–109. Digital Object Identifier: Doi: 10.1109/ICCSIT.2009.5234439.
[55] S. Yue, R.D. Santer, Y. Yamawaki, F.C. Rind, Reactive direction control for a mobile robot: a locust-like control of escape direction emerges when a bilateral pair of model locust visual neurons are integrated, Autonomous Robots 28 (2010) 151–167.
[56] S. Yue, F.C. Rind, Visually stimulated motor control for a robot with a pair of LGMD visual neural networks, Int. J. Adv. Mechatronics Syst. in press.

Shigang Yue is a Professor of Computer Science (July 2012) at the School of Computer Science, University of Lincoln, UK. He is the Founding Director of Computational Intelligence Laboratory (CIL) focusing on interdisciplinary research across Schools and Faculties at Lincoln. He received his B.Eng. Degree from Qingdao Technological University in 1988, M.Sc. and Ph.D. degrees from Beijing University of Technology (BJUT) in 1993 and 1996 respectively. He worked in BJUT as a Lecturer (1996) and promoted to an Associate Professor (1998). During 2000–2001, he was an Alexander von Humboldt Research Fellow working with Prof. Henrich in the Faculty of Computer Science, University

of Kaiserslautern, Germany. Before joining the University of Lincoln as a Senior Lecturer (September 2007) and promoted to a Reader (September 2010), he held research positions in University of Cambridge, University of Newcastle and University College London (UCL) respectively. His research interests are mainly within the field of artificial intelligence, computer vision, robotics, brains, and neuroscience. He is particularly interested in biological visual neural systems, evolution of neural subsystems and its applications in collision detection for vehicles, interactive systems and robotics. He has pioneered the area of using further organisations of directional selective neural networks for collision detection. He also has research interest in medical image analysis established in Cambridge. He has published more than 60 journals and conference papers in computer vision, artificial life, neural systems, neural evolution, vehicle collision detection, robotic navigation, robotic manipulation skills and dynamic simulations, many of them are in top tier high impact journals. He has chaired International Conferences on Natural Computation and Neural Networks, has been a reviewer for several reputable international journals and a committee member of several international conferences, and is coordinating several EU FP7 projects on bio-inspired neural computation, VLSI realisation and applications.

Dr. F. Claire Rind received the B.Sc. Degree in Animal Physiology from the University of Canterbury, Christchurch, New Zealand in 1976 and a Ph.D. in Zoology from Cambridge University, Cambridge, U.K. in 1982. She is currently a Reader in Invertebrate Neuroscience in the School of Biology and at the Institute of Neuroscience, Newcastle University, UK. Previously, she held a Royal Society University Research Fellowship and Biotechnology and Biological Sciences Research Council (BBSRC) Advanced Research Fellowship. Her current research interests include sensory processing by the insect brain, neuronal pathways for collision avoidance in locusts, bio-inspired robotics and Application Specific Integrated Circuits (ASICS) for visual tasks. Dr. Rind is a member of the Society for Experimental Biology, The Physiological Society, and the International Society for Neuroethology.